

## Sn-Zn-Ga-xPr 钎料组织与性能

李 阳<sup>1</sup>, 薛松柏<sup>1</sup>, 杨晶秋<sup>2</sup>, 叶 焕<sup>1</sup>, 陈 澄<sup>1</sup>, 顾立勇<sup>3</sup>, 顾文华<sup>3</sup>

(1. 南京航空航天大学 材料科学与技术学院, 南京 210016; 2. 哈尔滨焊接研究所, 哈尔滨 150080;

3. 常熟市华银焊料有限公司, 常熟 215513)

**摘 要:** 研究了添加合金元素 Ga 及稀土元素 Pr 对 Sn-Zn 钎料组织与性能的影响。适量添加锆, 可以提高钎料的润湿性能; 但当锆含量超过 0.12% (质量分数) 时, 锆会在钎料表面形成氧化渣, 恶化钎料的润湿性能。锆的添加可以改善焊点的力学性能, 抗剪强度在锆含量为 0.08% 时增加至最大。锆加入后细化了钎料基体中的富锌相, 当锆含量不超过 0.08% 时, 界面层平整且厚度变化不大, 但若稀土添加过量, 则界面层会明显增厚。锆在 Sn9Zn0.5Ga 钎料中的最佳添加量为 0.08% 左右。

**关键词:** SnZn 钎料; 润湿性; 力学性能; 显微组织

**中图分类号:** TG454 **文献标识码:** A **文章编号:** 0253-360X(2012)05-0033-04



李 阳

## 0 序 言

在传统的电子行业中, Sn-Pb 钎料是一种广泛应用于微电子封装的钎焊连接材料。然而, 含铅钎料的大量使用, 会给生态环境带来严重的破坏。因此开发无铅钎料来替代传统的锡铅钎料已经成为世界关注的热点课题。

目前, Sn-Zn 系合金被认为是最有希望替代 Sn-Pb 钎料的无铅钎料之一, 其最吸引人的地方就是共晶熔点接近 SnPb 焊料, 可直接采用现行的工艺流程, 且力学性能优良、成本低廉、资源丰富<sup>[1]</sup>。但其润湿性较差, 阻碍了它的发展。通过研究已发现<sup>[2]</sup>, Ga 元素添加后会改善 SnZn 钎料的润湿性能, 在添加量为 0.5% (质量分数) 时, 润湿性能最好, 且组织均匀, 晶粒得到明显的细化, 焊点力学性能最佳。已有研究发现<sup>[3,4]</sup>, 锆加入后可细化钎料基体中的富锌相, 减缓界面金属间化合物( IMC) 层的生长速度, 且抑制了 IMC 与铜基板界面 CuSn 化合物形成, 使得界面组织更为稳定, 提高了焊点可靠性。

文中以 Sn9Zn0.5Ga 为基体, 添加稀土元素 Pr, 研究其对 Sn9Zn0.5Ga 钎料润湿性、焊点力学性能的影响, 通过研究不同含量锆对 Sn9Zn0.5Ga 钎料组织的影响, 揭示锆对 Sn9Zn0.5Ga 钎料性能的影响规律。

## 1 试验方法

### 1.1 试验材料和合金的熔炼以及制备

试验采用 Sn9Zn0.5Ga 无铅钎料为基体, 添加的锆含量见表 1。

表 1 试验编号及锆含量(质量分数, %)

Table 1 Compositions of solder alloys

编号	1	2	3	4	5	6	7
锆的加入量	0.020	0.040	0.080	0.120	0.250	0.50	0.75
锆的实测量	0.018	0.039	0.082	0.118	0.251	0.49	0.74

为了尽可能的保证所添加元素的含量的精准度, 试验利用 Sn5Pr 中间合金, 将一定比例混合的原材料放入氧化铝陶瓷坩埚中置于井式炉加热熔化, 加热到 900 ℃ 左右, 待全部熔化后保温 1 h。此外, 为了防止锌及锆的氧化, 在冶炼过程中采用质量比为 1.3:1 的 KCl + LiCl 熔盐进行保护, 并通入氮气。熔炼完成后随炉冷却浇注成 40 mm 左右的钎料条。

### 1.2 润湿性能测试

润湿性能测试采用日本 RHESCA 公司的 SAT-5100 型可焊性测试进行。该测试仪依据润湿平衡法原理测试钎料的润湿性能。试验过程参照日本工业标准 JIS Z3198: 2003《无铅钎料实验方法—第四部分: 基于润湿平衡及触角法的润湿性实验方法》进行, 试验参数按照上述标准进行设定, 浸入深度为 2 mm, 浸入速度为 5 mm/s, 浸入时间为 10 s。

### 1.3 力学性能试验

为模拟实际生产,试验采用 PCB 基板为锡镀层的焊盘、0805 片式电阻元器件进行焊接,片式电阻焊点的剪切力采用日本 RHESCA 公司 STR-4000 型微焊点强度测试仪来测试。试验依据日本工业标准 JIS Z 3198—2003,《无铅钎料试验方法—第七部分:片式元件焊点的剪切试验方法》的规定<sup>[5]</sup>来测试。

### 1.4 界面显微组织观察试样制备

Sn9Zn0.5Ga-xPr/Cu 界面试样是通过钎料在铜片上的铺展制得的。将事先准备好的铜片和钎料按顺序放置温度为 250 °C 的电阻炉中,保持 300 s 后,取出冷却。将上述试样沿对角线方向剪开,得到钎料与基体的界面,磨平、镶样,经砂纸打磨抛光后用 4% HNO<sub>3</sub> 酒精腐蚀,进行界面组织的观察。

## 2 试验结果和分析

### 2.1 润湿性能

依照 1.2 节所述试验标准,在 225 °C 下分别测试了 7 种不同镧添加量的钎料合金的润湿时间和润湿力,测定结果如图 1 所示。

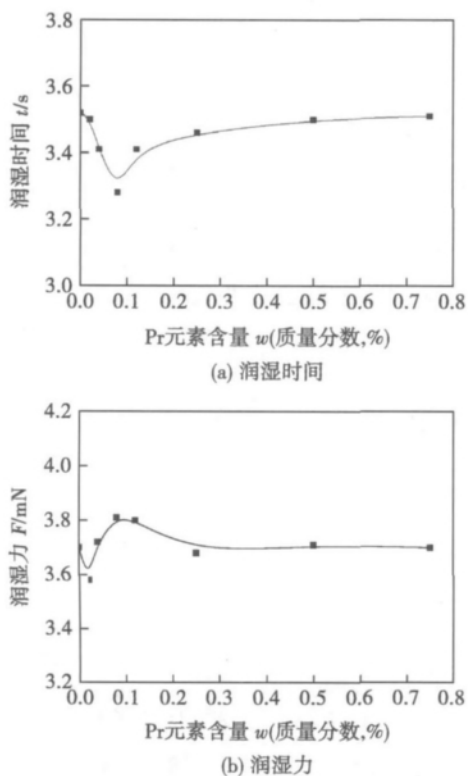


图 1 Sn9ZnGa-xPr 钎料润湿性能 (ZnCl<sub>2</sub> + NH<sub>4</sub>Cl)

Fig. 1 Wetting properties of Sn9ZnGa-xPr lead-free solders (ZnCl<sub>2</sub> + NH<sub>4</sub>Cl)

由图 1 可知,当向 Sn9Zn0.5Ga 钎料中添加的

稀土元素 Pr 不超过 0.08% 时,熔融钎料对铜基板的润湿力随镧含量的增加有略微回落后,在总趋势上表现出明显的增加,在镧含量为 0.08% 时润湿力达到最大值。此后,随镧含量的进一步增加,钎料润湿性能下降,当镧添加量超过 0.25% 时,润湿力降低至与 Sn9Zn0.5Ga 基体钎料相当。润湿性能的另外一个评价标准,润湿时间随镧含量的增加呈先减小后增大的趋势,在镧含量为 0.08% 时,达到最大值。

稀土元素 Pr 之所以能有效改善钎料的润湿性能,其原因在于稀土元素是表面活性元素,适量镧的添加会有效降低液态钎料的表面张力,从而提高钎料的润湿性能。而过量 Pr 元素的加入则会因其被过度氧化而导致钎料表面张力的增大,从而使其润湿性能减弱。

### 2.2 焊点的力学性能

Sn9Zn0.5Ga-xPr 焊点的剪切力如图 2 所示。

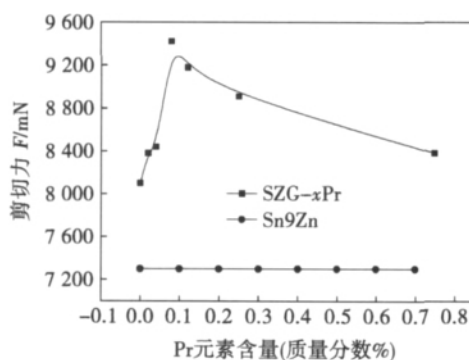


图 2 稀土镧添加量对焊点力学性能的影响

Fig. 2 Mechanical properties of Sn9Zn lead-free soldered joints with addition of Pr

从图 2 曲线可以看出,焊点的剪切力先是随着镧含量的增加而增加,在镧含量为 0.08% 时达到最大值,此时,焊点的剪切力比未添加稀土时提高了 14.8%,比 Sn9Zn 提高了 30.14%。随着镧含量的进一步增加,焊点的剪切力反而下降,但总体来说添加稀土镧后焊点的剪切力有所提高。

图 3 为钎料合金显微组织。由 3 图可知,当稀土元素添加量很少时,钎料组织表现为典型的 Sn-Zn 共晶组织。即在  $\beta$ -Sn 基体上分布着黑色的针状乃至棒状的富锌相<sup>[5]</sup>,如图 3a 所示。另外,钎料中所添加的 0.5% 的 Ga 元素固溶于钎料基体中与晶界处<sup>[6,7]</sup>。当镧添加量在 0.02% ~ 0.08% 范围内时,钎料中的富锌相的尺寸随着镧含量的增加而减小,且分布更为均匀,当镧含量为 0.08% 时显微组织最为细小均匀,如图 3b 所示。根据细晶强化理论,

其强度应为最高,这与文中试验结果吻合。随后随着镨含量的进一步增加,钎料中开始出现小块的黑色物质,钎料焊点力学性能开始下降。镨含量进一步增加

时,黑色物质有聚集长大的趋势,焊点力学性能显著下降。对图 3c 中黑色物质进行 EDS 分析发现此黑色物质为 Sn-Pr 化合物,Sn 与 Pr 的原子比约为 3:1。

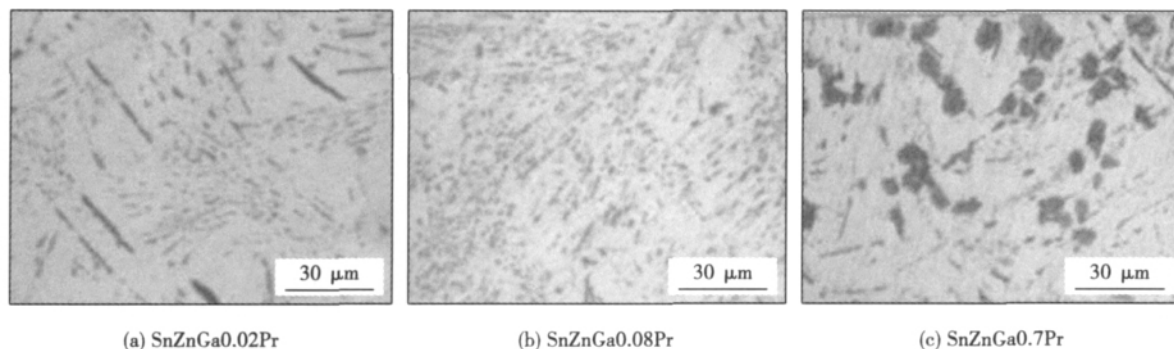


图3 Sn9Zn0.5Ga-xPr 钎料合金显微组织

Fig. 3 Microstructure of Sn9Zn0.5Ga-xPr lead-free solders

### 2.3 稀土镨对 SnZnGa-xPr/Cu 界面组织的影响

图 4 为 SnZnGa0.08Pr/Cu 焊点焊后界面组织形貌。可以看出,钎焊后钎料与铜基板之间形成了一层平坦的 IMC 层。经 EDS 分析发现此金属间化合物仅含 Cu 和 Zn 元素,Cu 与 Zn 的原子比为 35.39:64.51,接近于 5:8。

图 5 为不同镨含量钎料在铜基板上的焊后界面组织形貌。可以发现,当镨的含量在 0.02% ~ 0.08% 之间时,虽然钎料基体组织越来越均匀、细小,但界面处 IMC 的形貌及厚度变化不大。但当镨的添加量增加至 0.12% 时,IMC 的厚度明显增加,并且在界面附近出现了黑色稀土相聚集的现象。镨

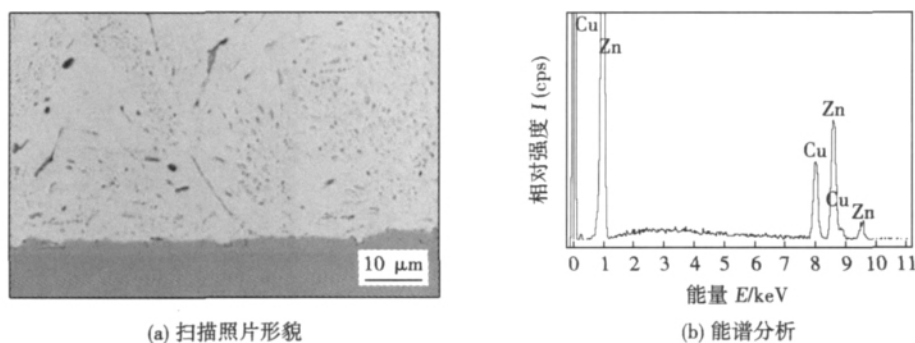


图4 SnZnGa0.08Pr/Cu 的界面显微组织

Fig. 4 Interface microstructure of SnZnGa0.08Pr/Cu lead-free solder

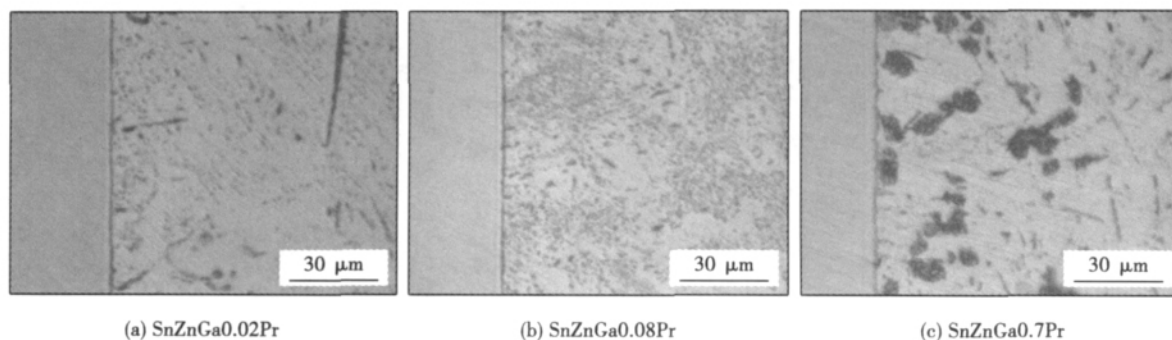


图5 不同镨含量钎料在铜基板上的焊后界面组织形貌

Fig. 5 Interface morphology after welding with different Pr content solder on Cu substrate

含量越多,这一现象越明显,且原来在钎料基体中分布比较均匀的稀土相在经过钎焊后出现了明显的向界面迁移的现象。

钎料与铜基板的反应过程中,由于锌的活性,液态钎料中的 Zn 原子会率先与铜基板发生反应形成 Cu-Zn 化合物,随后,由于锌在锡中的扩散速度较快,靠近界面处的钎料中的 Zn 原子不停地向铜片扩散,同时,铜片上的 Cu 原子也不断向界面扩散,最后在界面处形成了图 4 中所示的连续的 Cu-Zn 化合物层,而靠近界面侧的钎料中的富锌相明显减少。因此 SnZnGa-xPr/Cu 焊后界面产物为  $\text{Cu}_5\text{Zn}_8$ 。

前面分析发现,当锆含量不超过 0.08% 时,界面平整且厚度变化不大,但若稀土添加过量,则界面层会明显增厚。众所周知,过厚的金属间化合物层会降低焊点的结合强度。所以稀土锆的最佳添加量应维持在恒量。对于过量稀土元素导致界面层变厚的原因,初步分析认为这可能是由于 Sn-Pr 相的吉布斯形成能比 Zn-Pr 相低很多,添加一定量的 Pr 元素以后,锆的亲锡效应使得更多的锌向界面处富集并与铜反应生成 Cu-Zn 化合物相,因而界面处 IMC 的厚度有所增大。

### 3 结 论

(1) 在 Sn9Zn0.5Ga 钎料中加入稀土锆后,钎料的润湿性能随着锆含量的增加而提高,在添加量为 0.08% 时达到最大值。随后,随着锆含量的进一步增加,钎料由于 Pr 元素的过度氧化,润湿性能反而有所下降。

(2) 焊点的抗剪力先是随着锆含量的增加而增加,在锆含量为 0.08% 时达到最大值,此时,焊点的剪切力比未添加稀土时提高了 14.8%;随后随着锆含量的进一步增加,焊点的剪切力反而下降,但总体来说添加稀土锆后焊点的剪切力有所提高。

(3) 当锆添加量在 0.02% ~ 0.08% 范围内时,钎料中的富锌相的尺寸随着锆含量的增加而减小,且分布更为均匀,当锆含量为 0.08% 时显微组织最为细小均匀。随着锆含量的进一步增加,钎料中开

始出现小块的  $\text{PrSn}_3$  相黑色物质,锆含量进一步增加时,黑色物质有聚集长大的趋势。

(4) 当锆的含量在 0.02% ~ 0.08% 之间时,界面处 IMC 的形貌及厚度变化不大。但当锆的添加量增加至 0.12% 时,IMC 的厚度明显增加,并且在界面附近,出现了黑色稀土相聚集的现象。锆含量越多,这一现象越明显。

### 参考文献:

- [1] McConnack M, Jin S, Kammlott G W. The design of new Pb-free solder alloys with improved properties [C] // IEEE International Symposium on Electronics and the Environment, USA, 1995: 171-176.
- [2] Chen Wenxue, Xue Songbai, Wang Hui, *et al.* Effects of Ga on properties of Sn-9Zn lead-free solder [J]. Transactions of the China Welding Institution, 2008, 29(4): 37-40.
- [3] Xiao Zhengxiang. Effect of Pr on the microstructure and properties of Sn-9Zn lead-free solder [D]. Nanjing: Nanjing University of Aeronautics and Astronautics, 2011.
- [4] 王春青,李明雨,田艳红,等. JIS Z 3198 无铅钎料试验方法简介与评述 [J]. 电子工艺技术, 2004, 25(3): 50-54.  
Wang Chunqing, Li Mingyu, Tian Yanhong, *et al.* Review of JIS Z 3198: test method for lead-free solders [J]. Electronics Process Technology, 2004, 25(3): 50-54.
- [5] 吴文云,邱小明,殷世强,等. Bi, Ag 对 Sn-Zn 无铅钎料性能与组织的影响 [J]. 中国有色金属学报, 2006, 16(1): 158-163.  
Wu Wenyun, Qiu Xiaoming, Yin Shiqiang, *et al.* Influence of Bi, Ag on microstructure and properties of Sn-Zn lead-free solder [J]. The Chinese Journal of Nonferrous Metals, 2006, 16(1): 158-163.
- [6] Chen K I, Lin K L. The microstructures and mechanical properties of the Sn-Zn-Ag-Al-Ga solder alloys—the effect of Ga [J]. Journal of Material Science: Material in Electronics, 2007, 18(1/3): 77-91.
- [7] Chen Wenxue, Xue Songbai, Wang Hui, *et al.* Investigation on properties of Ga to Sn-9Zn lead-free solder [J]. Journal of Material Science: Material in Electronics, 2010, 21(5): 496-502.

作者简介: 李 阳,女,1988 年出生,硕士研究生。主要从事微电子组装与封装研究。Email: renee881028@126.com

通讯作者: 薛松柏,男,教授。Email: Xuesb@nuaa.edu.cn

ing strength; CuCrZr alloy

#### **Efficient numerical simulation and experimental study on residual stress induced by GMAW with cable-type wire**

FANG Chenfu<sup>1</sup>, WANG Haisong<sup>1</sup>, LIU Chuan<sup>1</sup>, HU Qingxian<sup>1</sup>, SHI Zhen<sup>2</sup> ( 1. School of Material Science and Engineering, Jiangsu University of Science and Technology, Zhenjiang 212003, China; 2. Jiangsu victor hi-tech welding industry Co., LTD., Huai'an 223100, China) . pp17 – 20

**Abstract:** Gas metal arc welding (GMAW) with cable-type wire is an innovative welding method which provided prominent advantages of high efficiency and low power consumption. Until now, it has rare report on the welding residual stress of the new welding method. In the present study, the heat source model based on the welding seam profile is adopted to efficiently simulate the welding temperature field, and it is validated by comparison of simulated temperature field and experimental welding seam profile of bead-on-plate welding through GMAW with single wire. In addition, the simulated residual stress results are compared with the experimental ones on the top surface obtained by the hole drilling method. The investigated results show that the heat source model based on the weld seam profile is suitable for efficient temperature field simulation of GMAW with cable-type wire; on the top surface within the welding line and adjacent region, the residual stress distribution and magnitude of GMAW with cable-type wire are almost identical to those of submerged arc welding (SAW) under the same welding specifications, however, in the region far from the welding line, the amplitude of longitudinal compressive residual stress induced by GMAW with cable-type wire is larger than that induced by SAW.

**Key words:** cable-type welding wire; gas metal arc welding; residual stress; efficient numerical simulation

#### **Effects of thermal aging on intermetallic compounds and properties of Cu/Al brazing joint**

JI Feng<sup>1</sup>, XUE Songbai<sup>1</sup>, ZHANG Man<sup>1</sup>, LOW Jiyuan<sup>2</sup>, WANG Shuiqing<sup>2</sup> ( 1. College of Materials Science and Technology, Nanjing University of Aeronautics and Astronautics, Nanjing 210016, China; 2. Zhejiang Xinrui Welding Material Co. Ltd, Shaoxing 312400, China) . pp 21 – 24

**Abstract:** Cu/Al dissimilar metals were joined with Zn-22Al filler metal by torch-brazing technology and heat treated at constant temperature of 250 °C for 0 to 1000 h. To guarantee the reliability of the Cu/Al torch-brazing joints in service requirement, the growth rate of intermetallic compounds on Cu side was calculated and the effects of the intermetallic compound layer on the electrical and mechanical properties have been investigated under various annealing time. It was observed that the width of intermetallic compound increased as the thermal aging proceeded, and the growth rate of the intermetallic compound was  $6.1 \times 10^{13} \text{ cm}^2/\text{s}$  when the aging temperature was 250 °C. A thicker intermetallic compound layers could degrade the resistivity and shear strength of Cu/Al joints. When the thickness of intermetallic compound was 4.2 μm and 18.1 μm, the electric resistance was 120.3 μΩ and 132.9 μΩ, respectively. Moreover, the shear strength of Cu/Al brazing joint increased by 3% when the aging time was 100 h while the strength decreased by 15% when

the Cu/Al joints endured 1000 h thermal aging.

**Key words:** Cu/Al brazed joints; thermal aging; resistivity; shear strength

#### **Numerical simulation on dynamic performance of assistant gas during laser cutting process**

TAN Xianghu<sup>1</sup>, WANG Wei<sup>2</sup>, SHAN Jiguo<sup>1,3</sup>, WAN Peng<sup>1,3</sup>, WANG Xuyou<sup>2</sup>, LIN Shangyang<sup>2</sup> ( 1. Department of Mechanical Engineering, Tsinghua University, Beijing 100084, China; 2. Harbin Welding Institute, China Academy of Machinery Science & Technology, Harbin 150080, China; 3. Key Lab for Advanced Materials Processing Technology, Ministry of Education, Beijing 100084, China) . pp 25 – 28

**Abstract:** The dynamic performance of assistant gas plays an important role on cutting kerf forming in laser cutting process. The VOF method and depth adaptive laser heat source were used to set up a multiphase flow model which can simulate the interaction between assistant gas and cutting kerf. Cutting experiments were carried out to verify this model. The cut kerf morphology, dynamic performance of assistant gas and temperature distribution were investigated from holing to stable cutting in the total cutting process. The calculation results show that the dynamic performance of assistant gas changes constantly during laser holing, which is affected by cutting frontier shape and cutting depth, etc. Assistant gas flow, cutting kerf morphology and temperature are no longer changing during stable cutting stage. The model can effectively reflect the cutting depth and width which are influenced by dynamic performance of assistant gas.

**Key words:** laser cutting; assistant gas flow field; numerical simulation; depth adaptive heat source

#### **Quantitative evaluation on metal transfer process stability of arc welding based on autocorrelation analysis**

GAO Liwen<sup>1,2</sup>, XUE Jiaxiang<sup>1</sup>, CHEN Hui<sup>1</sup>, ZHANG Xue<sup>1</sup>, Wang Ruichao<sup>1</sup> ( 1. School of Mechanical and Automotive Engineering, South China University of Technology, Guangzhou 510640, China; 2. College of Information Technology, Guangzhou University of Chinese Medicine, Guangzhou 510006, China) . pp 29 – 32

**Abstract:** This paper proposed a quantitative evaluation method based on autocorrelation analysis, to extract the coefficient of variation of intervals between autocorrelation function peaks from arc welding voltage and current signals, which were then used as the quantitative values to evaluate the metal transfer process stability in arc welding. Experiments showed that results obtained through this method were consistent with those from manual analysis. Besides, the combination of the quantitative values obtained through this method and other quantitative values has preferably realized the automatic evaluation of dynamic characteristics of power supply for CO<sub>2</sub> arc welding. The recognition accuracy reached 97.4359%, which was quite close to the standard of practical use.

**Key words:** metal transfer; stability; autocorrelation; quantitative

#### **Microstructure and properties of Sn-Zn-Ga-xPr lead-free solder**

LI Yang<sup>1</sup>, XUE Songbai<sup>1</sup>, YANG Jingqiu<sup>2</sup>, YE Huan<sup>1</sup>, CHEN Cheng<sup>1</sup>, GU Liyong<sup>3</sup>, GU Wenhua<sup>3</sup> ( 1. College

of Materials Science and Technology , Nanjing University of Aeronautics and Astronautics , Nanjing 210016 , China; 2. Harbin Welding Institute , Harbin 150080 , China; 3. Changshu Huayin Filler Metals Co. , Ltd , Changshu 215513 , China) . pp 33 – 36

**Abstract:** Effects of rare earth element Pr additions on the microstructure and properties of Sn-Zn-Ga solder were studied in this paper. The wettability of solder was significantly improved by 0.08% Pr addition. However, the wettability of solder would deteriorate when the Pr addition exceeds 0.12% due to the oxidization of Pr element at the liquid surface. Moreover, the mechanical property of solder joint was improved by Pr addition and the maximum shear strength was obtained when 0.08% Pr was added. The Zn-rich phase in the solder matrix was refined by Pr but the thickness of interface layer showed no obvious difference when Pr was less than 0.08%. When excessive Pr was added, the interface layer thickness of the joint increased significantly, so that the optimal content of Pr in the Sn<sub>9</sub>Zn<sub>0.5</sub>Ga solder is about 0.08%.

**Key words:** Sn-Zn fill metal; wettability; mechanical properties; microstructure

**Double-side friction stir welding of wear resistant aluminum silicon copper alloy** ZHANG Zhiyun , CHEN Maoai , WU Chuansong ( MOE Key Laboratory for Liquid-Solid Structural Evolution and Materials Processing , Shandong University , Jinan 250061 , China) . pp 37 – 40

**Abstract:** The 10 mm thick wear resistant Al-Si-Cu alloy plates were double-side friction stir welded ( D-FSW) . The microstructure and mechanical properties of the joints were investigated. The results show that the as-cast Al grain and Si reinforcement particles in the weld are remarkably refined during friction stir welding. The distribution of Si particles in the weld is more uniform than that in as-received base metal. The refinement of the grains and the uniformity of Si particles in the second pass are better than those in the first one. The joints of double pass welding in opposite direction ( OD joints) exhibit lower tensile strength than those of double pass welding in the same direction ( SD joints) . All the OD joints fractured through the advancing side of the joints , while the fracture paths of SD joints depend on the welding parameters. The tensile strength of SD joints welding at a stirring tool rotating speed of 950 rpm and a welding speed of 10 mm•min<sup>-1</sup> is up to 87.4% of the base metal.

**Key words:** double-side friction stir welding; Al-Si-Cu alloy; microstructure; grain refinement; tensile strength

**Study on friction stir welding of 2A97 Al-Li alloy** ZHANG Hua<sup>1,3</sup> , KONG Deyue<sup>2</sup> , CHEN Xuefeng<sup>2</sup> , CAO Jian<sup>3</sup> , ZHAO Yanhua<sup>2</sup> , HUANG Jihua<sup>1</sup> ( 1. School of Materials Science and Technology , University of Science and Technology Beijing , Beijing 100083 , China; 2. Capital Aerospace Machinery Company , Beijing 100076 , China; 3. State Key Lab of Advanced Welding and Joining , Harbin Institute of Technology , Harbin 100051 , China) . pp 41 – 44

**Abstract:** The weldability of 2A97 Al-Li alloy was studied using different friction stir welding variables in this paper. The results showed that the tensile strength and the elongation rate decreased with the increasing of the rotation speed. With the

increasing of the welding speed , the tensile strength firstly increased to a maximum value then decreased. The maximum tensile strength was 373 MPa , which reached to 69% of that of the base metal , when the rotation speed was 600 r/min and the welding speed was 200 mm/min. The joints were mostly fractured at the weld nugget. Most of the precipitated phases in the weld nugget and the heat affected zone were decomposed. The precipitate density in the heat affected zone was higher than that in the weld nugget.

**Key words:** Al-Li alloy; friction stir welding; microstructure; mechanical properties

**Numerical simulation of welding residual deformation in welded joints of marine steel plate by FEM** LU Xuedong<sup>1</sup> , WU Mingfang<sup>1</sup> , CENG Yue<sup>2</sup> , WANG Huan<sup>2</sup> , SHEN Songpei<sup>2</sup> ( 1. Jiang Su university of science and technology , Jiang Su , Zhenjiang 212003 , China; 2. HuDong-ZhongHua Ship Building Company Limited , Shanghai 200129 , China) . pp 45 – 48

**Abstract:** Using the three-dimensional finite element method , the residual deformation of joints obtained with the AH36 steel plate with thickness of 6 mm under different welding conditions was studied in this paper. The numerical simulation results showed that the longitudinal distortion and the angular distortion changed dramatically. As to different welding methods , the deformation was small when the unique CO<sub>2</sub> gas arc welding was used , while large deformation was found when the CO<sub>2</sub> arc and SAW were combined together. The residual deformation was controlled effectively by water cooling , especially for angular deformation with the unique CO<sub>2</sub> gas arc welding. To verify the finite element simulation results , an experiment using the same parameters was done. With some error , the experimental results were consistent with the numerical results , indicating that the welding deformation in different welding conditions can be simulated with the three-dimensional finite element method.

**Key words:** marine steel plate; residual deformation; water cooling; finite element modeling

**Interfacial microstructure and properties of SnCuNi-xPr/Cu solder joint** LUO Jiadong<sup>1</sup> , XUE Songbai<sup>1</sup> , YE Huan<sup>1</sup> , YANG Jingqiu<sup>2</sup> ( 1. College of Materials Science and Technology , Nanjing University of Aeronautics and Astronautics , Nanjing 210016 , China; 2. Harbin Welding Institute , Harbin 150080 , China) . pp 49 – 52

**Abstract:** Effects of rare earth element Pr on the intermetallics ( ZMC) between Sn<sub>0.7</sub>Cu<sub>0.05</sub>Ni-xPr lead-free solder and Cu substrate were studied in this paper. And the possible influence mechanism was initially introduced. The experimental results showed that the interface morphology was greatly modified and became more uniform and flat due to the addition of Pr , and the effect of 0.05% Pr addition was more remarkable than that of 0.15% Pr. Adding Pr could reduce the driving force and time of the interfacial reaction to restrain excessive IMC growth. It was concluded that there was a synergistic effect on the interfacial reaction between Pr and Ni. The strength and ductility of the solder joint were greatly improved due to the refined microstructure because of the pinning effect on the migration of grain boundaries brought by adding Pr , and precipitation hardening strengthened